THE GALAXY DISTRIBUTION SURROUNDING THE SCULPTOR VOID

GEORGE RHEE
New Mexico State University, Department of Astronomy, Box 30001/Department 4500, Las Cruces, New Mexico 88003

PETER KATGERT
Leiden Observatory, Postbus 9513, 2300 RA Leiden, The Netherlands
Received 13 September 1991; revised 21 January 1992

ABSTRACT

We present the results of a survey of galaxy redshifts toward the Sculptor void. Radial velocities for 113 galaxies in the right ascension range 22^h–2^h and declination range $-35°$ to $-25°$ have been obtained. This region is of interest since there are suggestions that it contains a two-dimensional sheet of galaxies at the interface between two voids. We have added our redshifts to the known redshifts in this area and have applied a statistical test to determine the nature of the galaxy distribution in this volume of space. The method is aimed at quantifying the topology of the distribution. The method yields quantitative results which are consistent with a distribution of sheets and voids.

1. INTRODUCTION

In this paper, we present the results of a redshift survey we have made towards the Sculptor void. In recent years, redshift surveys have revealed large structures in the galaxy distribution with a variety of topologies. The galaxy distribution has been described as filamentary or cellular (Einasto *et al.* 1980; Batuski & Burns 1985), sheetlike (Geller & Huchra 1989), bubblelike (de Lapparent *et al.* 1986), or "spongelike" in appearance (Gott *et al.* 1986), or some combination of these (Haynes & Giovanelli 1986; da Costa *et al.* 1988).

Observations of these large structures provide a powerful constraint on models of galaxy formation. The current, most popular model of galaxy formation has too little large scale power to account for a number of recent observations. One of the most troubling observations is the large coherence scale of peculiar velocity flows (Lynden-Bell *et al.* 1988), whose theoretical implications have been discussed by Kaiser (1988), Bertschinger & Juszkiewicz (1988), and Ostriker & Suto (1990). Further problematic observations include the high amplitude of the cluster–cluster correlation function (Bahcall & Soneira 1983; Klypin & Kopylov 1983), the angular correlation function of galaxies at large separations (Maddox *et al.* 1990), and the existence of large structures like the Perseus Pisces supercluster (Haynes & Giovanelli 1986, 1988), the Bootes void (Kirshner *et al.* 1987), and the "great wall" that dominates the northern sky in the extended CfA survey (Geller & Huchra 1989). Prior to the discovery of the great wall, the evidence for sheetlike structures in the galaxy distribution was circumstantial, since in the CfA slice redshift, surveys filamentary structures were observed. We thus decided to search for a sheetlike structure with a view to mapping it and providing direct evidence for sheets. We made a redshift survey in a $7° \times 6°$ area in a region where a large surface density of galaxies is present on the sky survey, and combine our data with data from the literature in a much larger area of $10° \times 60°$ centered on our smaller area.

Parker *et al.* (1987), using spectra from low dispersion UKST objective prism plates, have used the 4000 Å feature, when detectable, to measure galaxy redshifts to an accuracy of 0.01 in z. They scanned a $5.35° \times 5.35°$ field centered on 00^h00^m, $-35°00'$. They found evidence for a filamentary structure extended in declination and a low redshift enhancement extended perpendicular to the filament. This enhancement appeared sheetlike in projection, and we decided to further investigate it as a candidate for a sheet in redshift. While our survey was under way, Maurellis *et al.* (1990) published a study of this area based on redshifts compiled from the literature. They found evidence for a wall of galaxies 650 km/s thick 2000×2000 km/s wide, forming the interface to the Sculptor and Eridanus voids.

2. THE DATA

2.1 Observations

In order to further investigate this interesting region of the sky, we have measured radial velocities of 113 galaxies in the right ascension range 22^h–2^h and declination range $-35°$–$-25°$. We used the European Southern Observatory 1.5 m telescope. Two runs were made in 1988 August and 1989 August, respectively. We used a GEC chip with a readout noise of 12e with a Boller and Chivens spectrograph at the Cassegrain focus of the 1.5 m telescope. The spectra we obtained had 7 Å resolution. Initially, candidate galaxies for spectroscopy were selected by eye using film copies of the SERC IIIa-J Sky Survey. By the time our second run was due, the Surface Photometry Catalog of the ESO-Uppsala galaxies had been published and we used it to sheet candidates for spectroscopy. To narrow down the list of galaxies, we selected galaxies with $B_T < 15.0$. B_T is the total blue magnitude measured to $\mu_B \simeq 25$–26 [see Lauberts & Valentijn (1989) for the exact definition]. In total, we have obtained radial velocities for 113 galaxies, 8 of which are not in the LV catalog. Radial velocities were measured using the cross-correlation method of Tonry & Davis (1979) (see also Rhee & Katgert 1988). We used a spectrum of M32 as a template. The spectrum was obtained from Keel (1983), it was taken with an 8″ aperture using the image dissector scanner on the 1 m Nickel telescope at Lick Observatory. The data are listed in Table 1. We list the LV catalog number, right ascension, declination heliocentric radial velocity total B and R magnitudes.

In Table 2 we compare our radial velocities with previously measured radial velocities. The velocities are taken from two sources. We searched the LV (1989) catalog and the catalog of da Costa *et al.* (1991) for galaxies with previously measured redshifts. There are 8 galaxies in the LV catalog

 0004-6256/92/051438-05$00.90

TABLE 1. The sample.

Object	α (1950) H	M	S	δ (1950) °	M	v	σ_v	B_T	R_T
4090100	0	1	44	-30	10.1	19398	135	15.25	14.52
4090130	0	2	27	-30	47.1	8154	114	15.00	13.62
4090140	0	2	58	-30	51.9	8495	112	15.28	14.10
4720180	0	9	42	-27	28.0	10383	100	14.99	13.71
4732100	0	16	28	-23	09.5	7393	91	14.65	13.72
4730250	0	29	21	-26	59.8	7266	133	14.68	13.05
4740070	0	35	21	-26	55.4	5649	167	14.81	13.56
4740270	0	44	44	-26	39.3	5645	202	14.88	13.58
2950060	0	45	58	-38	30.4	4948	102	14.42	13.17
3510110	0	48	40	-32	41.6	9657	100	14.69	13.05
4120010	0	57	50	-31	4.8	9711	263	14.72	13.69
4120070	1	6	24	-28	50.9	5012	131	13.50	11.71
4120140	1	9	59	-32	19.6	9201	111	15.06	13.69
4120160	1	10	36	-31	42.9	5483	120	14.57	13.22
3520220	1	11	24	-34	10.7	10025	285	15.12	14.05
3520241	1	11	38	-32	54.6	10016	245	15.29	14.55
4750150	1	13	23	-27	6.4	3531	180	14.08	12.67
3520550	1	19	14	-33	25.1	10808	121	14.28	12.99
3520570	1	19	44	-34	27.5	5600	141	14.63	13.39
4130050	1	23	18	-30	37.5	9150	60	14.17	12.89
4760180	1	28	54	-27	7.0	5775	153	14.49	13.03
3530290	1	36	13	-33	51.7	8911	47	14.75	13.58
4130190	1	38	3	-29	10.0	5618	126	13.71	12.60
3530310	1	38	21	-33	52.4	8670	102	14.98	13.45
4130200	1	38	23	-32	4.4	5979	122	14.05	13.28
4140010	1	43	37	-29	17.3	5779	74	14.82	13.18
4770070	1	47	6	-26	59.6	5898	177	14.85	13.42
4770090	1	47	33	-26	31.9	9537	157	14.76	13.76
4140050	1	47	34	-27	42.8	4134	87	14.56	13.05
4770140	1	52	42	-26	15.8	8827	81	14.52	12.77
4140200	1	56	55	-28	3.1	4473	220	14.70	13.49
4770200	1	58	18	-25	17.6	4181	114	14.71	13.22
4770210	1	58	32	-25	16.1	4415	88	14.07	12.49
4770220	1	59	13	-25	9.9	22815	160	14.52	13.03
4140270	2	02	29	-29	32.5	5080	181	14.46	13.03

TABLE 1. (continued)

Object	α (1950) H	M	S	δ (1950) °	M	v	σ_v	B_T	R_T
4670081	22	4	2	-31	18.0	9772	94	14.93	13.94
5320210	22	5	25	-25	18.4	5553	203	14.65	13.47
5320260	22	8	5	-25	19.2	5042	190	14.71	13.25
4670240	22	11	12	-29	37.9	4498	222	13.31	12.49
4670300	22	12	5	-28	10.9	4039	99	14.37	13.31
5330070	22	13	46	-27	4.2	8214	88	14.34	13.32
4670420	22	16	25	-28	39.2	8485	235	14.28	13.26
5330140	22	17	2	-26	35.6	2636	142	13.75	12.95
4050090	22	17	34	-32	56.3	16911	183	14.87	13.79
5330180	22	19	31	-27	8.1	5749	162	14.86	13.64
4670460	22	19	51	-32	27.1	8341	85	14.60	13.13
5330240	22	20	55	-26	52.0	7582	70	14.19	13.13
4670580	22	23	16	-31	7.4	8541	86	14.86	13.44
4670620	22	24	4	-31	8.5	33696	157	14.94	14.44
4670650	22	24	54	-30	17.7	8461	133	14.64	13.96
5330350	22	27	21	-27	1.8	10002	92	14.68	13.30
4680130	22	30	57	-27	30.2	6887	81	14.34	13.71
4050290	22	31	13	-32	39.3	23383	26	14.61	14.19
4680160	22	33	21	-31	59.2	8016	85	14.67	13.66
5340100	22	36	06	-25	58.2	3390	173	13.90	12.11
4060100	22	42	4	-34	28.5	8791	130	14.97	14.76
4060370	22	56	22	-34	20.6	8964	62	14.99	13.94
4070020	23	1	56	-34	19.6	1727	170	14.08	12.84
4690120	23	4	24	-28	53.0	9678	97	15.28	14.10
4700020	23	19	53	-29	33.3	6879	97	14.70	13.23
RK105	23	22	28	-31	25.9	10668	102		
4700110	23	26	56	-29	6.4	7244	117	14.91	13.55
RK99	23	33	37	-31	52.7	14871	112		
4710020	23	38	17	-28	37.0	8339	160	14.51	0.00
RK112	23	38	52	-29	35.9	15685	110		
RK113	23	38	58	-29	30.8	15209	130		
RK115	23	39	14	-28	18.1	8599	180		
RK111	23	39	39	-30	28.5	18936	150		
4710070	23	41	48	-31	57.5	11099	100	15.19	13.94
4080240	23	42	2	-34	46.0	11745	90	15.20	13.90

TABLE 1. (continued)

Object	α (1950) H	M	S	δ (1950) °	M	v	σ_v	B_T	R_T
RK108	23	42	17	-32	21.3	18733	220		
4710090	23	43	11	-29	47.7	10494	98	13.85	12.38
4710110	23	43	47	-28	17.0	8418	140	15.24	13.85
4710111	23	43	47	-28	16.8	8493	116	14.77	13.53
4710120	23	44	00	-29	20.9	10466	90	14.50	13.06
4710130	23	44	02	-28	59.2	19073	190	15.60	14.09
RK102	23	44	24	-29	26.9	10251	20		
4710140	23	44	39	-28	14.1	8479	70	14.69	13.40
4710170	23	44	53	-28	23.2	8224	152	14.03	12.55
4710180	23	45	9	-27	45.9	8873	156	14.94	13.84
4710190	23	45	9	-28	25.0	8623	90	13.42	11.99
RK94	23	45	09	-28	24.9	8070	120		
4710200	23	45	15	-30	48.0	2984	125	12.10	11.11
4710220	23	46	39	-30	31.5	13747	70	14.65	13.43
4710230	23	46	40	-29	18.5	10569	165	14.97	13.78
4710240	23	47	16	-28	13.7	8925	60	14.74	13.36
RK12	23	48	03	-28	42.7	8698	111		
RK33	23	48	34	-31	37.0	13489	140		
RK6	23	49	19	-28	11.5	8835	112		
4710280	23	49	20	-30	52.5	14896	130	14.88	13.95
RK17	23	49	35	-29	21.5	8770	90		
4710320	23	49	47	-30	30.5	8660	73	14.74	13.58
RK16	23	49	49	-29	18.2	8716	105		
RK23	23	49	50	-29	54.5	13016	130		
4710340	23	49	56	-30	27.5	8877	107	14.33	13.20
RK10	23	50	09	-28	50.9	17703	200		
4710360	23	50	37	-32	0.0	14425	108	15.17	13.76
RK21	23	50	50	-29	48.9	8753	120		
4710390	23	51	51	-29	9.9	8683	80	15.29	13.95
RK27	23	53	15	-30	08.8	8655	152		
4710450	23	53	49	-31	37.9	8695	130	14.18	12.81
4710471	23	53	51	-29	18.1	8909	130	14.69	13.33
4710480	23	54	22	-32	24.7	8867	200	14.96	14.19
4710500	23	55	25	-30	8.7	8899	85	14.84	13.53
RK45	23	55	20	-32	05.6	8653	95		

TABLE 1. (continued)

Object	α (1950) H	M	S	δ (1950) °	M	v	σ_v	B_T	R_T
4710510	23	55	43	-30	23.3	8988	75	14.83	13.82
RK52	23	56	05	-30	07.3	8827	70		
4710540	23	56	45	-32	0.6	8360	66	14.75	13.78
4090010	23	58	45	-27	41.8	8168	116	14.92	13.42
4090070	23	59	59	-30	54.0	8971	80	14.50	13.20

TABLE 2. Previously measured redshifts.

Object	α (1950) H	M	S	δ (1950) °	M	v_{RK}	σ_{vRK}	v_{LV}	σ_{vLV}
4710090	23	43	11	-29	47.7	10494	98	10380	100
4710100	23	43	40	-28	22.6	8418	140	8392	10
4710140	23	44	39	-28	14.1	8479	70	8560	14
4710170	23	44	53	-28	23.2	8224	152	8272	10
4710190	23	45	09	-28	25.0	8662	90	8631	10
4710200	23	45	15	-30	48.0	2984	125	2968	8
4710220	23	46	39	-30	31.5	13747	70	13809	33
4710510	23	55	43	-30	23.3	8988	75	9086	25
4739250	00	29	21	-26	59.8	7266	133	7235	45
5320260	22	08	05	-25	19.2	5042	190	4892	29
4670240	22	11	12	-29	37.9	4498	222	4303	15
4670300	22	12	05	-28	10.9	4039	99	4062	21
4690120	23	04	24	-28	53.0	9678	97	9701	35
4710020	23	38	17	-28	37.0	8339	160	8418	38
4710090	23	43	11	-29	47.7	10494	98	10380	20

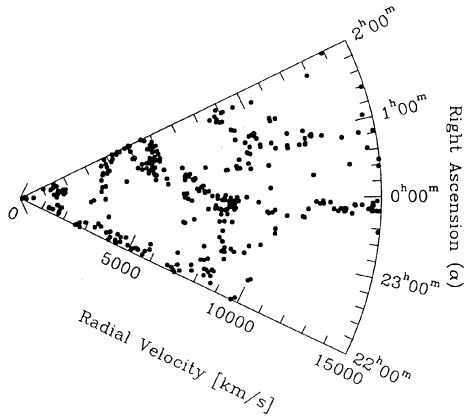

FIG. 1. Wedge plot of the galaxy distribution in our survey. The right ascension range is $22^h < \alpha < 2^h$, the declination range $-35 < \delta < -25$, and the redshift range is $0 < z < 15\,000$ km/s.

and 7 galaxies in the da Costa *et al.* catalog for which we have determined radial velocities. For the 8 LV galaxies, we find that the mean difference between our measured redshifts and the LV redshifts is − 13 km/s. The rms difference is 68 km/s. For the 7 galaxies from the da Costa catalog, we have a mean difference of 52 km/s and a rms difference of 108 km/s. For the joint sample of 15 galaxies, we find a mean difference of 17 km/s and a rms difference of 89 km/s. These results are consistent with our error estimates for the redshifts of these galaxies, which vary between 70 and 152 km/s with a mean of 102 km/s.

2.2 The Database

The goal of this project is to characterize the galaxy distribution surrounding the Sculptor void. In order to produce as complete a database as possible for studying the distribution of galaxies, we have combined the redshifts we obtained with those available from the literature. The two sources we used are the ESO-UPPSALA catalog and the compilation of Fairall (1988). We also searched the Abell *et al.* (1989) catalog for the presence of rich clusters in the surveyed volume. In total, we have 465 galaxies in the surveyed volume and 3 rich Abell clusters with measured redshifts.

Figures 1 and 2 display the data we obtained, combined with already available data. The dataset we examine is 10° slice centered on $\delta = -30$, spanning the right ascension range 22^h–2^h, and radial velocity range 0–15 000 km/s. Figure 1 shows a wedge plot of the data. Figure 2 shows an equal area projection map of the galaxies shown in Fig. 1. Adopting the void nomenclature of Maurrelis *et al.* (1990), we see in Fig. 1 the Sculptor void extending from 3000 to ~9000 km/s. At 2000 km/s, we have the Eridanus void which borders on the Sculptor void.

2.3 Completeness of Sample

Ideally, when undertaking a redshift survey, one would like to take a galaxy photometric catalog and measure radial velocities of galaxies complete to a given magnitude limit. Projects using dedicated 4 m class telescopes with multifiber spectrographs are being initiated both in the northern and southern hemispheres. In view of the lack of a published photometric catalog in the southern sky, we have selected galaxies from the Lauberts–Valentijn catalog (1989), which contains all galaxies on the ESO quick blue survey plates with a maximum angular diameter of 1′. Since this is the only published galaxy catalog in the southern sky, we describe the completeness of our survey in terms of this catalog. The number of galaxies from the Lauberts–Valentijn catalog in the region $22^h \leqslant \alpha \leqslant 2^h$; $-35° \leqslant \delta \leqslant -25°$ is 738. With a limited amount of access to national facilities, we were not able to measure the radial velocities of all the galaxies in the LV catalog in this region. We find that to a B_T magnitude of 15.0 the survey is complete to 80%. To the LV data, we have added galaxies from the literature with measured redshifts falling in the relevant right ascension and declination range. The main source from which we have added data is the compilation of Fairall (1988). Maurellis *et al.* suggest that redshift measurements are susceptible to selection effects in direction not in redshift. They have compared the *sky* coverage of the Fairall (1988) compilation with that of the LV catalog. By this, they mean that the ratio of Fairall galaxies to LV galaxies does not vary greatly from one ESO Schmidt plate field to another. We thus conclude that we are reasonably complete to a magnitude of B_T of 15.0 in the LV sample. We also conclude that our adding galaxies from the literature compilation of Fairall has not introduced a significant bias in our data, since the sky coverage of this latter sample is similar to that of the LV sample.

3. ANALYSIS

We have applied the topology method to characterize the galaxy distribution surrounding the Eridanus void. This method provides a quantitative description of the topology of the galaxy distribution. The method is based on an analy-

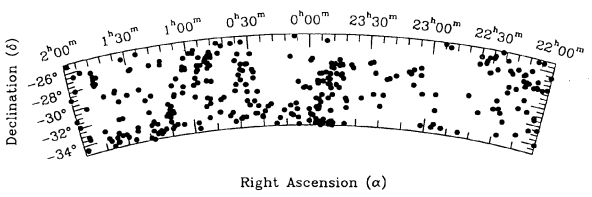

FIG. 2. Equal area projection of the galaxies in the sample.

sis of the density contour surfaces of the smoothed density distribution (Gott *et al.* 1986).

Gott *et al.* (1986) have developed a method for quantifying the topology of the galaxy distribution. The method has been described in a clear manner by Melott (1990) and Gott (1988). In particular, Melott's review is accompanied by a number of figures that greatly help clarify the concepts of topology. We summarize the salient features of the method below. The goal of the method is to characterize the topology of the galaxy distribution revealed by redshift surveys. The first step is to smooth the data (points in α, δ, v_r space) to produce a density field. A contour at constant density of this field produces a two-dimensional surface. This surface may have various topological characteristics. For example, it may be spongelike, in which case the matter and voids are interlocking and the surface displays a high degree of connectivity. At the other extreme, the surface may consist of a number of isolated lumps in an empty background, in which case it has a low degree of connectivity. This latter case is referred to by Melott (1990) as a meatball topology. Gott *et al.* (1986) have shown that one can quantify the topology of a surface using one number; the genus. The genus of an arbitrary surface with holes and disconnected pieces is: g = number of holes − number of isolated regions. By holes we do not mean voids in the cosmological sense but rather in a topological sense, an example of which is the hole in a doughnut. An algorithm has been developed for estimating g for a given density contour (Weinberg 1988). The algorithm is based on the Gauss–Bonnet theorem, which relates the gaussian curvature of a surface to the number of holes in the surface. The conventional wisdom in cosmology is based on the assumption that the structure we see in the galaxy distribution today was produced by the growth after recombination of random phase Gaussian fluctuations with a power spectrum $P(k)$. In the linear regime, fluctuations grow in place, simply increasing in amplitude, and the density contour surfaces as a function of ν (the number of standard deviations by which the contour threshold density is above or below the average density) do not change. Hamilton *et al.* (1986) give an analytical expression for the genus per unit volume as a function of ν. A key result is that while the amplitude of the genus curve depends on the power spectrum $P(k)$, the shape of the curve is independent of the power spectrum. The analytical result shows that the $\nu = 0$ contour is always spongelike, while for $|\nu| > 1$ isolated clusters and voids are seen depending on whether ν is positive or negative.

One can then compare the observed genus curve from the redshift surveys with that expected on the basis of Gaussian fluctuations. A bubblelike distribution of galaxies would produce a genus curve $g(\nu)$ shifted to lower ν relative to the predicted curve for Gaussian fluctuations. This would indicate an excess of isolated regions at low ν and connected contours at high ν.

As explained in Sec. 2, the data we have obtained are redshifts measured in a slice. Melott *et al.* (1989) have shown how the genus method can be extended to analyze a galaxy distribution sampled in two dimensions. Park *et al.* (1991) have applied this method to the slice data of de Lapparent *et al.* (1986) and Karachentsev & Kopylov (1990).

To deal with two-dimensional distributions, the genus method must be generalized from three to two dimensions and a subtle point arises. In three dimensions, we can imagine either isolated clusters in a low density background, isolated voids in a high density background, or the third symmetric alternative of a sponge topology. In two dimensions, a closed curve necessarily divides space into an inside and outside and the sponge alternative does not exist. Melott *et al.* have shown that one can extend the genus method to two dimensions by referring to isolated high- and low-density regions, rather than voids and holes. $g(\nu)$ is now defined as the number of isolated high density regions − number of low density regions. A consequence of this definition of $g(\nu)$ is that the genus curve for a two-dimensional gaussian field is antisymmetric. As the density threshold is raised from the mean, the number of separate high-density regions will, at first, increase. As the density threshold is lowered from the mean, the number of isolated low-density regions will increase. For a Gaussian random density field, the mean two-dimensional genus per unit area is:

$$g(\nu) = \frac{1}{(2\pi)^{3/2}} \frac{\langle k^2 \rangle}{2} \nu e^{-\nu^2/2},$$

where ν is the threshold level in units of the standard deviation of the density fluctuations and $\langle k^2 \rangle$ is the mean square of the wave number for a given power spectrum $P(k_x, k_y)$.

Clearly the two-dimensional method is less powerful than the three-dimensional approach in discriminating between various topologies. However, Melott *et al.* have shown, by comparing the analytic formula with the results of toy models and N-body simulations, that the method can yield useful results. By measuring the $g(\nu)$ curve from the data, one can see if the analytical form shown above is valid. If the curve deviates from the form shown above, one can, by comparing with simple models, infer how the observed galaxy distribution deviates from the Gaussian model.

We have applied the method described above to our data. The data must first be smoothed before the genus contours can be determined. We have chosen a smoothing radius of 650 km/s and a maximum radius of 15 000 km/s for the sample. The smoothing radius is determined by the requirements that it be larger than the mean galaxy separation at $r_{\min}$ and $r_{\max}$ (where these minimum and maximum distances correspond to the limits of the survey) and that it maximize the number of independent resolution elements.

To estimate errors, 12 samples were generated from the original data using the bootstrap method described by Barrow *et al.* (1984). The bootstrap method involves generating pseudo-datasets from the original dataset. To generate a pseudo dataset, one labels the galaxies in the original sample 1 to N. One then generates a set of N numbers randomly chosen between 1 and N. The N random numbers indicate which galaxies are selected to be in the pseudo-dataset. The net result is that some galaxies in the original set are selected more than once while some are completely omitted. Strong structures consisting of many galaxies will not be affected much, while weak structures will often change.

Twelve samples were generated from the original sample in this manner. Using these 12 samples, the mean genus and 1σ scatter as a function of ν could be calculated. These are shown in Fig. 3 together with the original data. The solid curve is the theoretical curve (see above equation) fit to the average of the bootstrap runs. Examining Fig. 3, we find three regimes. Around the median contour in the regime $|\nu| < |0.5|$, we see that the data are shifted to the right relative to the theoretical curve. This suggests that we are seeing an excess of isolated low-density regions or bubblelike voids. Melott *et al.* (1989) have generated a toy bubble distribu-

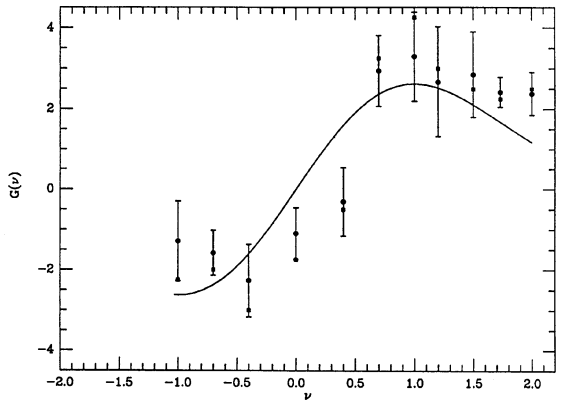

FIG. 3. The genus measured from our redshift data. Open squares are the genus from the original sample and filled dots and error bars are the mean and 1σ variation in 12 bootstrap replacement runs. The solid curve is the theoretical curve fit to the average genus from the bookstrap runs.

tion, where particles are placed on the surfaces of irregular space-filling polyhedra. Similar shift to the right of the $g(\nu)$ curve is observed [see their Figs. 4(a) and 4(b)]. In addition to the observed curve not passing through the origin, the toy model curve shows a sharper transition from positive to negative genus than the analytical gaussian curve and a slower falloff to zero at negative ν. These two properties are also observed in our data. In the high density regime ($\nu > 0.5$), we find a reasonable fit to the $g(\nu)$ curve.

To summarize, we find that our data deviate from the predicted curve for a two-dimensional Gaussian random field in three similar ways to that of a curve produced by slices through a toy model. The toy model is generated by placing particles on the surfaces of irregular space filling polyhedra. This result suggests that we are sampling a similar sheet like distribution in our data.

4. CONCLUSIONS

We have investigated the galaxy distribution surrounding the Sculptor void. We have added 113 redshifts to the known redshifts in this region. To determine the nature of the topology of the galaxy distribution in this region, we have applied the topology method. The method we have applied involves calculating the genus (a topological measure) of contours of the density field. The density field is derived from the data by smoothing with a Gaussian. By comparing the observed genus for varying density contours with that expected for a gaussian field we find objective evidence for the existence of a topology of galaxies in sheets surrounded by voids.

It is a pleasure to thank Rien van de Weygaert and Adrian Melott for helpful discussions. Bob Donahue provided much help with the plotting software at NMSU. We enjoyed the able assistance of Hector Vega and Helmut Herborn at the 1.5 m telescope.

REFERENCES

Abell, G. O., Corwin, H. G., & Olowin, R. P. 1989, ApJS, 70, 1
Bahcall, N., & Soneira, R. 1983, ApJ, 270, 20
Batuski, D. J. & Burns, J. O. 1985, ApJ, 299, 5
Bertschinger, E., & Juszkiewicz, R. 1988, ApJ, 334, L 59
Barrow, J. D., Bhavsar, S. P., & Sonoda, D. M. 1984, MNRAS, 210, 19p
da Costa, L. N., *et al.* 1988, ApJ, 327, 544
da Costa, L. N., Pellegrini, P. S., Davis, M., Meiksin, A., Sargent, W. L. W., & Tonry, J. 1991, ApJS, 75, 935
de Lapparent, V., Geller, M. J., & Huchra, J. P. 1986, ApJ, 302, L 1
Einasto, J., Joeveer, M., & Saar, E. 1980, MNRAS, 193, 353
Fairall, A. P. 1988, MNRAS, 230, 69
Geller, M. J., & Huchra, J. P. 1989, Science, 246, 897
Gott, J. R., Melott, A. L., & Dickinson, M. 1986, ApJ, 306, 341
Gott III, J. R., 1988, PASP, 100, 1307
Hamilton, A. J. S., Gott, J. R., & Weinberg, D. H. 1986, ApJ, 309, 1
Haynes, M. P., & Giovanelli, R. 1986, ApJ, 306, L55
Haynes, M. P., & Giovanelli, R. 1988, in Large Scale Motions in the Universe, Pontifical Academy of Sciences Study Week, No. 27, edited by V. Rubin and G. Coyne (Specola Vaticana, Rome), p. 31
Kaiser, N. 1988, MNRAS, 231, 149
Karachentsev, I. D., & Kopylov, A. I. 1990, MNRAS, 243, 390
Keel, W. C. 1983, ApJ, 269, 466
Kirshner, R. P., Oemler, A., Schechter, P. L., & Schectman, S. A. 1987, ApJ, 314, 493
Klypin, A. A., & Kopylov, A. I. 1983, SvAL, 9, 41
Lauberts, A., & Valentijn, E. A. 1989, The Surface Photometry Catalogue of the ESO-Uppsala Galaxies (European Southern Observatory, Garching)
Lynden-Bell, D., Faber, S. M., Davies, R. L., Dressler, A., Terlevich, R., & Wegner, G. 1988, ApJ, 326, 19
Maddox, S. J., Efstathiou, G., Sutherland, W. J., & Loveday, J. 1990, MNRAS, 242, 43 P
Maurellis, A., Fairall, A. P., Martravers, D. R., & Ellis, G.F.R. 1990, A&A, 229, 75
Melott, A. L. 1990, Phys. Rep., 193, 1
Melott, A. L., Cohen, A. P., Hamilton, A. J. S., Gott III, J. R., & Weinberg, D. H. 1989, ApJ, 345, 618
Ostriker, J. P., & Suto, Y. 1990, ApJ, 348, 378
Park, C., Gott III, J. R., Melott, A. L., & Karatchensev, I.D. 1991, preprint
Parker, Q. A., Beard, S. M., & MacGillivray, H. T. 1987, A & A, 173, L 5
Rhee, G. F. R. N., & Katgert, P. 1987, A&AS, 72, 243
Tonry, J., & Davis, M. 1979, AJ, 84, 1511
Weinberg, D. H. 1988, PASP, 100, 1373